Atmospheric
Chemistry
and Physics
Discussions

1 **Urban increments of gaseous and aerosol pollutants and**

2 **their sources using mobile aerosol mass spectrometry**

3 **measurements**

4 **M. Elser[1], C. Bozzetti[1], I. El-Haddad[1], M. Maasikmets[2], E. Teinemaa[2], R. Richter[1],**

5 **R. Wolf[1], J.G. Slowik[1], U. Baltensperger[1] and A.S.H. Prévôt[1]**

6 [1]{Laboratory of Atmospheric Chemistry, Paul Scherrer Institute, 5232, Villigen PSI,

7 Switzerland}

8 [2]{Estonian Environmental Research Centre, 10617, Tallinn, Estonia}

9 Correspondence to: I. El-Haddad (imad.el-haddad@psi.ch) and A. S. H. Prévôt

10 (andre.prevot@psi.ch)

11

12 **Abstract**

13 Air pollution is one of the main environmental concerns in urban areas, where anthropogenic

14 emissions strongly affect air quality. This work presents the first spatially-resolved detailed

15 characterization of the $PM_{2.5}$ in two major Estonian cities (Tallinn and Tartu), using mobile

16 measurements. In both cities, the non-refractory (NR)-$PM_{2.5}$ was characterized by a high-

17 resolution time-of-flight aerosol mass spectrometer (HR-ToF-AMS) using a recently

18 developed lens which increases the transmission of super-micron particles. Equivalent black

19 carbon (eBC) and several trace gases including carbon monoxide (CO), carbon dioxide (CO_2)

20 and methane (CH_4) were also measured. The chemical composition of the $PM_{2.5}$ was found to

21 be very similar in the two cities. Organic aerosol (OA) constituted the largest fraction,

22 explaining on average about 52 to 60 % of the $PM_{2.5}$ mass. Four sources of OA were

23 identified using positive matrix factorization (PMF): hydrocarbon-like OA (HOA, from

24 traffic emissions), biomass burning OA (BBOA, from biomass combustion), residential

25 influenced OA (RIOA, probably mostly from cooking processes with possible contributions

26 from waste and coal burning) and oxygenated OA (OOA, related to secondary aerosol

27 formation). OOA was the major OA source during night-time, explaining on average half of

28 the OA mass, while during day-time mobile measurements the OA was affected by point

29 sources and dominated by the primary fraction. A strong increase in the secondary organic

30 and inorganic components was observed during periods with transport of air masses from

Atmospheric
Chemistry
and Physics
Discussions

1   polluted continental areas, while the primary local emissions accumulated during periods

2   with temperature inversions. Mobile measurements offered the identification of different

3   source regions within the urban areas and an accurate calculation of the urban increments.

4   HOA, eBC, CO_2 and CO showed stronger enhancements on busy roads during the morning

5   and evening traffic rush hours; BBOA had its maximum enhancement in the residential areas

6   during the evening hours and RIOA was enhanced in both the city center (emissions from

7   restaurants) and in the residential areas (emissions from residential cooking). In contrast,

8   secondary components (OOA, SO_4, NO_3, NH_4, and Cl) had very homogeneous distributions

9   in time and space. We were able to determine a total $PM_{2.5}$ urban increment in Tartu of 6.0

10    $\mu g\ m^{-3}$ over a regional background concentration of 4.0 $\mu g\ m^{-3}$ (i.e., a factor of 2.5 increase).

11   Traffic exhaust emissions were identified as the most important source of this increase, with

12   eBC and HOA explaining on average 53.3 and 20.5 % of the total increment, respectively.

13

1   Introduction

15   Atmospheric particulate matter (PM) plays a central role in many environmental processes

16   through its influence on climate (radiative forcing; Myhre et al., 2013), the hydrological cycle

17   (Ramanathan, et al., 2001) and its adverse effects on health (Pope and Dockery, 2006).

18   Recently, major attention has been devoted to the study of the $PM_{2.5}$ fraction (particulate

19   matter with an aerodynamic equivalent diameter $d_{aero} \leq 2.5\ \mu m$), which has been linked to

20   increased lung cancer rates (Hu and Jiang, 2014), acute bronchitis and asthma (Gao et al.,

21   2015), and mortality (Dockery et al 1993; Laden et al., 2006). Atmospheric particles can be

22   classified as primary or secondary aerosols according to their formation processes. Primary

23   particles are directly emitted, while secondary aerosols are formed from gas-phase precursors

24   following chemical transformation in the atmosphere. Aerosols can be further classified in

25   terms of their emission sources as natural sources (e.g. volcanic eruptions, wildfires, sea salt,

26   dust or biogenic emissions from plants) or anthropogenic sources (mostly from combustion

27   processes, e.g. traffic and residential wood combustion).

28   Due to enhanced contributions of anthropogenic sources, air quality is commonly lower in

29   urban areas compared to rural or suburban locations (Putaud et al., 2004). In Europe, annual

30   average $PM_{2.5}$ mass concentrations in urban areas commonly vary between a few $\mu g\ m^{-3}$ up to

31   35 $\mu g\ m^{-3}$ (Putaud et al., 2010). The predominance of specific aerosol sources (e.g.

32   residential, traffic, industry) or the implementation of new technologies (e.g. car fleet, heating

1   systems, etc.) may strongly influence the levels and physicochemical characteristics of the

2   pollutants in these locations. Moreover, certain orographic features and stagnant

3   meteorological conditions may induce the accumulation of local pollutants (Putaud et al.,

4   2004; Carbone et al., 2010; Squizzato et al. 2012). Likewise, long-range transport of

5   continental air masses has been shown to influence the PM in different urban areas in Europe

6   (Niemi et al., 2009; Baker, 2010; Salvador et al., 2013; Beekmann et al., 2015; Di Gilioa et

7   al., 2015; Ulevicius et al., 2015). While the PM levels and physicochemical properties of the

8   particles are well characterized in Western Europe, data are scarce in Eastern European cities,

9   especially in the Baltic region, hindering air quality assessment and quantification of the main

10   aerosol sources.

11   In contrast to conventional stationary measurements, mobile measurements (including

12   zeppelin, aircraft and ground measurements) are suited for pollutant mapping, chasing of

13   mobile sources or measurements in emission plumes, etc. Ground-based measurements by

14   mobile platforms have been successfully performed in the last years to measure particles and

15   trace gases from real-world traffic emissions (Pirjola et al., 2004, 2006 and 2012; Kwak et al.,

16   2014; Kyung Hwan et al., 2015) and from wood burning emissions (Pirjola et al., 2015).

17   More recently, aerosol mass spectrometers (AMS) have been deployed in mobile laboratories

18   in order to determine the physical and chemical properties of submicron aerosols (PM_1,

19   particulate matter with aerodynamic equivalent diameter $d_{aero} \leq 1$ μm) in urban environments

20   like Zurich (Mohr et al., 2011), Paris (Von der Weiden-Reinmueller et al., 2014a and 2014b)

21   or Barcelona (Mohr et al., 2015). Moreover, a newly developed inlet for the AMS has been

22   used to measure the chemical composition of the non-refractory (NR)-$PM_{2.5}$ fraction in

23   Bologna (Wolf et al., 2015).

24   In this work we present the first detailed in-situ mass spectrometric measurements of air

25   pollutants in the two biggest cities in Estonia (Tallinn and Tartu). The measurements were

26   performed using the Paul Scherrer Institute (PSI) mobile laboratory (Bukowiecki et al., 2002;

27   Mohr et al., 2011; Wolf et al., 2015). The use of a high-resolution time-of-flight aerosol mass

28   spectrometer (HR-ToF-AMS) with a novel $PM_{2.5}$ lens allowed for a detailed characterization

29   of the NR-$PM_{2.5}$ fraction in the measurement areas. The spatial distributions of the sources of

30   organic aerosols (OA), inorganic aerosols (nitrate (NO_3), sulfate (SO_4), ammonium (NH_4),

31   and chloride (Cl)), equivalent black carbon (eBC) and some of the major gas-phase

32   components (carbon monoxide (CO), carbon dioxide (CO_2) and methane (CH_4)) were

33   determined in the urban areas. Such analyses allowed for the calculation of regional

Atmospheric
Chemistry
and Physics
Discussions

Open Access

EGU

1   background and urban concentrations of the different gas- and particle-phase components and

2   provided direct insights into the spatial resolution of local emissions and their impact on the

3   air quality in different city areas. Long-range transport of pollutants and accumulation events

4   as well as their effect on the particle- and gas-phase mass concentrations will also be

5   discussed.

6

7   **2   Methodologies**

8   **2.1   Measurement campaign**

9   The measurements were performed in the two biggest cities in Estonia. Tallinn, the capital

10   and the largest city of Estonia, has a population of 413,000 inhabitants (Statistical Database,

11   2015) and occupies an area of 158.3 km^2. Located on the northern coast of the country,

12   Tallinn has some of the biggest ports in the Baltic Sea. Among them, the old city harbor is

13   one of the busiest passenger harbors in the region. Tartu, with 38.8 km^2 and more than 97,000

14   inhabitants in 2015 (Statistical Database, 2015), is the second largest city in Estonia. The city

15   is situated in the center of southern Estonia, in the post-glacial valley of the Emajõgi River,

16   which influences the local meteorological conditions and favors the accumulation of local

17   pollutants under frequent temperature inversions. Previous studies identified traffic emissions

18   and residential heating as the major sources of air pollution in these two cities (Urb et al.,

19   2005; Orru et al., 2011). An older vehicle fleet, the limited network capacity of the city

20   streets (which generates congestions during rush hours) and the extensive use of studded

21   tires, have been reported to strongly enhance the effect of the traffic emissions in the city

22   center and major roads. Residential heating includes extensive use of inefficient wood and

23   coal stoves with low stacks in both cities. In this regard, a detailed modeling study performed

24   in Tallinn and Tartu (Orru et al., 2011) revealed that the city centers and the neighborhoods

25   with local heating are exposed to much higher average $PM_{2.5}$ concentrations compared to

26   other areas of the cities.

27   The measurements took place from 10 to 17 March 2014 in Tartu and from 25 March to 1

28   April 2014 in Tallinn. The GPS trace of the driving routes in the two cities is shown in Fig. 1.

29   The paths were chosen in order to cover heavily trafficked roads, residential areas where

30   different heating systems are used (wood/coal burning, central heating or mixed) and

31   background sites with little local emissions. In Tallinn, streets close to the old town harbor

32   were also included in the route. To obtain statistically significant spatial distributions of the

Atmospheric
Chemistry
and Physics
Discussions

1   major pollutants, 25 loops were performed at each location throughout the measurement

2   periods at different times of the day. The average loop duration was about 72 minutes in

3   Tartu and 112 minutes in Tallinn. Stationary measurements were typically performed

4   overnight at a gasoline station in Tartu (influenced by city center and residential emissions)

5   and at the Estonian Environmental Research Centre (EERC) in Tallinn (a background site).

6   Meteorological data were recorded in a meteorological-tower in Külitse (around 10 km south-

7   east from Tartu) and in the Tallinn-Zoo meteorological station.

8   **2.2   Mobile laboratory set-up**

9   A schematic of the instrumental set-up in the PSI mobile platform is shown in Fig. S1. The

10   main inlet of the mobile platform was kept at a constant flow of ~11 m sec^{-1} for isokinetic

11   sampling during driving conditions, assuming an average velocity in the city of ~ 40 km h^{-1}.

12   Two different inlet lines connected the main inlet to the aerosol and gas-phase

13   instrumentation. The deployed instruments, measured parameters and their time resolution

14   are listed in Table 1. All parameters were determined with high time resolution (between 1

15   and 25 seconds), critical for the identification of source regions using a mobile platform.

16   An HR-ToF-AMS (Aerodyne Research Inc.) was deployed to measure the chemical

17   composition of the NR-PM$_{2.5}$ aerosol, including NO_3, SO_4, NH_4, Cl, and OA. For this work

18   the AMS was equipped with a recently developed aerodynamic lens which extends the

19   measured particle size to the PM$_{2.5}$ fraction (in contrast to the conventional PM$_1$ lens). The

20   PM$_{2.5}$ lens efficiently transmits particles between 80 nm and up to at least 3 μm and has been

21   well characterized by Williams et al. (2013) and tested in previous chamber and ambient

22   studies (Wolf et al., 2015; Elser et al., 2015). The operating principle of the instrument can be

23   found elsewhere (DeCarlo et al., 2006). A nafion drier (Perma Pure MD-110) was set before

24   the AMS inlet in order to dry the ambient particles and reduce uncertainties in the bounce-

25   related collection efficiency (CE$_b$) and possible transmission losses of large particles at high

26   relative humidity (RH).

27   A 7-wavelength Aethalometer (Magee Scientific, model AE33) was used to measure the

28   aerosol light absorption and to determine the equivalent black carbon (eBC) concentrations.

29   The measurement at 7 different wavelengths (370, 470, 520, 590, 660, 880 and 950 nm)

30   covers the range between ultraviolet and infrared and allows for the source apportionment of

31   different eBC fractions (Sandradewi et al., 2008; Zotter et al., in prep). Moreover, the dual

Atmospheric
Chemistry
and Physics
Discussions

1   spot measurement method corrects automatically for the loading effect and provides a real-

2   time calculation of the loading compensation parameter (Drinovec et al., 2015).

3   The concentrations of trace gases, including CO, CO_2 and CH_4 were measured by two

4   different analyzers (Picarro-G2301 and Licor-6262). In addition, some important parameters

5   for mobile measurements (GPS, temperature, relative humidity and solar radiation) were also

6   measured continuously.

2.3 AMS data analysis

7

8   AMS data were analyzed in Igor Pro 6.3 (WaveMetrics) using the standard ToF-AMS Data

9   Analysis toolkit (SQUIRREL version 1.53G and PIKA version 1.12G). Based on standard

10   NH_4NO_3 calibrations, the ionization efficiency (IE, defined as ions detected per molecules

11   vaporized) was determined to be $5.08 \cdot 10^{-8}$ (average of five calibrations during the full

12   measurement period). Standard relative ionization efficiencies (RIE) were used for nitrate,

13   chloride, and organics (RIE = 1.1, 1.3, and 1.4, respectively) and experimentally determined

14   for sulfate and ammonium (RIE = 1.11 and 4.29, respectively). A composition dependent

15   collection efficiency (CE) algorithm by Middlebrook et al. (2012) was used to calculate the

16   ambient mass concentrations.

2.4 Source apportionment techniques

17

2.4.1 OA source apportionment

18

19   To identify and quantify the major sources of OA in the different measurement areas, positive

20   matrix factorization (PMF; Paatero and Tapper (1994)) was applied to the highly time

21   resolved AMS data (see Table 1). The analysis were performed using the multilinear engine

22   tool (ME-2; Paatero, 1997) implemented in the Source Finder interface (SoFi; Canonaco et

23   al., 2013) coded in Igor Wavemetrics.

24   PMF is a bilinear unmixing algorithm which, as defined in Eq. (1), allows representing a two-

25   dimensional matrix of measured data ($\mathbf{X}$) as a linear combination of a given number of static

26   factors profiles ($\mathbf{F}$) and their corresponding time series ($\mathbf{G}$). The matrix $\mathbf{E}$ in Eq. (1) contains

27   the model residuals. The model uses a least squares approach to iteratively minimize the

28   object function Q described in Eq. (2):

29   $$\mathbf{X} = \mathbf{GF} + \mathbf{E} \qquad\qquad (1)$$

1
$$Q = \sum_{i=1}^{m} \sum_{j=1}^{n} \left(\frac{e_{ij}}{\sigma_{ij}} \right)^2 \qquad (2)$$

2   where e_{ij} are the elements from the error matrix (E) and σ_{ij} are the respective uncertainties of

3   **X**.

4   In our case, the model input consists of a data and error matrix of OA mass spectra, where the

5   rows represent the time series (62665 points, with steps of 25 seconds) and the columns

6   contain the ions fitted in high resolution (292 ions). The organic mass obtained from the high

7   resolution fits (up to m/z 115) agrees with the mass from the unit mass resolution fits (up to

8   m/z 737) within ± 5 %. The initial error values were calculated with the HR-AMS data

9   analysis software PIKA. A minimum error corresponding to the measurement of a single ion

10   was applied (Ulbrich et al., 2009). All variables with signal-to-noise ratio (SNR) lower than

11   0.2 were removed and the variables with SNR between 0.2 and 2 were down-weighted by

12   increasing their error by a factor of 3 (Paatero and Hopke, 2003). Moreover, all variables

13   directly calculated from the CO_2^+ in the organic fragmentation table (i.e. O^+, HO^+, H_2O^+ and

14   CO^+) (Allan et al., 2004) were excluded for the PMF analysis to appropriately weight the

15   variability of CO_2^+ in the algorithm and were reinserted post-analysis.

16   The possibility of local minima in the solution space and the uncertainty of the PMF solution

17   were investigated by means of bootstrap analysis. This statistical method is based on the

18   creation of replicate datasets perturbing the original data by resampling. In each replicate,

19   some randomly chosen rows of the original matrix are present several times, while other rows

20   do not occur at all (Paatero et al., 2014), such that the dimension of the data matrix is kept

21   constant. This resulted in about 64 % of the original points being used in each replicate. PMF

22   was applied to 100 different replicates and the variations among these results were used to

23   estimate the uncertainty of the initial PMF solution. Note that as each bootstrap run is started

24   from a different initialization point and hence this methodology includes the investigation of

25   the classic seed variability. All convergent solutions were found to be consistent, an

26   indication of the robustness of the chosen solution.

27   The results presented in this section were obtained by merging the measurements from the

28   two measurement locations, as no major changes were observed if the source apportionment

29   was performed for the individual cities.

1   2.4.2   eBC source apportionment

2   The Aethalometer measurements can be used to separate eBC from wood burning (eBC_{wb})

3   and from traffic (eBC_{tr}), by taking advantage of the spectral dependence of absorption, as

4   described by the Ångström exponent (Ångström, 1929). This method is described in detail in

5   Sandradewi et al. (2008) and has been successfully applied at many locations across Europe.

6   For a proper separation of the eBC fractions, the Aethalometer data was averaged to 30

7   minutes in order to increase the signal to noise. Thus, the obtained fractions eBC_{wb} and eBC_{tr}

8   could only be used for the correlations with the external tracers, but their spatial distributions

9   couldn't be explored. The absorption Ångström exponent was calculated using the absorption

10   measured at 470 and 950 nm and Ångström exponents of 0.9 and 1.7 were used for traffic

11   and wood burning, respectively, following the suggestions in Zotter et al. (In prep.).

12

13   **3   Results and discussion**

14   **3.1   Pollutant concentrations and temporal variability**

15   The temporal variation of all measured gas- and particle-phase components is shown in Fig.

16   2a. The type of measurement is indicated by different background colors (transparent for

17   stationary measurements and orange for mobile measurements). The measurement period

18   included three distinct meteorological periods of transport of polluted air masses and

19   accumulation of local emissions. These periods are referred to as special events (indicated by

20   a red frame) and will be treated separately and discussed in detail in Section 3.4. While the

21   AMS and Aethalometer were running almost continuously during the entire measurement

22   period, there is a small gap in the CO_2, CO and CH_4 data due to an instrument malfunction.

23   Over the full measurement period, the average mass concentration of $PM_{2.5}$ (NR-$PM_{2.5}$ plus

24   eBC) was 12.3 µg m^{-3}. In the gas-phase, average concentrations of 414.1 ppm of CO_2, 0.24

25   ppm of CO and 1.92 ppm of CH_4 were measured. In contrast to these relatively low average

26   values, extremely high concentrations were often recorded during the mobile measurements

27   due to local emissions from point sources (around 50 spikes with $PM_{2.5}$ mass concentration

28   exceeding 100 µg m^{-3}). Such intermittent pollution plumes (expected in some areas in a city)

29   cannot be detected from stationary measurements at an urban background site, but enhance

30   negative health impacts. As shown in Fig. 2b, neglecting the periods defined as special

31   events, the $PM_{2.5}$ average concentrations and relative contributions of the particle phase

Atmospheric
Chemistry
and Physics
Discussions

1   species were very similar at the two locations. If we compare day-time (07:00 to 19:00, local

2   time (LT)) and night-time (19:00 to 07:00, LT) measurements, in both cities the average

3    $PM_{2.5}$ was higher during the day (11.0 µg m^{-3} in Tartu and 11.6 µg m^{-3} in Tallinn) than during

4   the night (6.5 µg m^{-3} in Tartu and 7.1 µg m^{-3} in Tallinn), despite the development of the

5   boundary layer and increased dilution during day-time. OA constituted in all cases the largest

6   mass fraction, explaining on average 52.2 and 54.3 % of the $PM_{2.5}$ mass in Tartu (during

7   night- and day-time, respectively) and 55.2 and 60.1 % in Tallinn (during day- and night-

8   time, respectively). Primary emissions of eBC contributed on average 20.4 % and 33.7 % in

9   Tartu (during night-time and day-time, respectively), and 13.4 and 26.9 % in Tallinn (during

10   night-time and day-time, respectively), constituting a substantially higher fraction than at

11   other European locations (Putaud et al., 2010). The remaining mass, 12 to 28 %, was related

12   to secondary inorganic species, mostly ammonium sulfate and nitrate. These species were

13   found to be neutralized within the uncertainties (ratio of NH_4 expected from an ion balance to

14   NH_4 measured of 1.05, with R^2=0.95). During night-time a decrease in the relative

15   contribution of eBC was observed in favor of an enhanced contribution of the inorganic

16   species.

3.2 Sources of OA

18   To properly represent the temporal variations of the OA, four factors were required:

19   hydrocarbon-like OA (HOA), biomass burning OA (BBOA), residential influenced OA

20   (RIOA) and oxygenated OA (OOA). The mass spectra of these factors are reported in Fig. 3.

21   HOA is a primary source related to traffic emissions and its mass spectrum is characterized

22   by the presence of alkyl fragment signatures (Ng et al., 2011), with prominent contributions

23   of non-oxygenated species at m/z 43 ($C_3H_7^+$), m/z 55 ($C_4H_7^+$) and m/z 57 ($C_4H_9^+$). As shown

24   in Fig. S2, a fairly good correlation is found between HOA and eBC_{tr} (R^2 = 0.4). Moreover,

25   the ratio of HOA to eBC_{tr} was 0.5, which is in good agreement with previous European

26   studies (El Haddad et al., 2013 and references therein). BBOA is associated with domestic

27   heating and/or agricultural biomass burning activities, and shows characteristic high

28   contributions of the oxygenated hydrocarbons at m/z 60 ($C_2H_4O_2^+$) and m/z 73 ($C_3H_5O_2^+$),

29   which are known fragments from anhydrous sugars (Alfarra et al., 2007). BBOA correlates

30   fairly well with eBC_{wb} (R^2 = 0.4), and the ratio of BBOA to eBC_{wb} was 4.0 (Fig. S2), which

31   within the method uncertainties is consistent with previously reported values (Crippa et al.,

32   2013). The ratio BBOA to eBC_{wb} was found to be very sensitive to the chosen Ångström

Atmospheric
Chemistry
and Physics
Discussions

1   exponent for traffic, and it increased to 4.8 if a slightly higher Ångström exponent (i.e. 1.0

2   instead of 0.9) was considered for traffic. RIOA is a hydrocarbon-rich factor that was

3   required for a reasonable explanation of the variability in the data. Due to its increase in the

4   residential areas, this factor was associated with residential emissions. Given its strong

5   correlation ($R^2 = 0.9$) with cooking markers such as the fragment ion $C_6H_{10}O^+$ at m/z 98 (Sun

6   et al., 2011; Crippa et al., 2013), we expect that a great part of this factor is related to cooking

7   emissions (see Fig. S2). Moreover, as in previously reported cooking spectra (Mohr et al.,

8   2012), the RIOA mass spectrum shows a higher m/z 55 to m/z 57 ratio than HOA. However,

9   in the absence of diurnal trends due to the driving conditions, the separation of cooking

10   emissions from other residential emissions (such as domestic coal and waste burning) was not

11   possible. OOA is associated with aged emissions and secondary organic aerosol formation,

12   and its profile is characterized by a very high m/z 44 (CO_2^+). In general, OOA increases

13   simultaneously with the secondary species (especially NO_3), but the ratio among these

14   components changes during special events (Fig. S2). If the number of factors is decreased,

15   the RIOA factor is not resolved and the OOA time-series becomes contaminated by local

16   spikes, which is unexpected for a regional component (see Fig. S3 and S4). In contrast, if a

17   five-factor solution is considered an additional highly oxygenated factor is obtained

18   ("unknown" factor in Fig. S3 and S4). The mass spectrum of this additional factor resembles

19   a low-volatility OOA (LV-OOA), as resolved in many previous works (Jimenez et al., 2009),

20   but its time series exhibits the typical characteristics of the primary factors, i.e. strong

21   increases in emission areas. Therefore, this further increase in the number of factors doesn't

22   seem to improve the interpretation of the data, as the new factor cannot be explicitly

23   associated to distinct sources or processes. Accordingly, a four-factor solution was

24   considered as optimal and is utilized below.

25   Figure 4a represents the time series of the absolute mass (top panel) and relative contributions

26   (bottom panel) of the retrieved OA sources for the two measurement locations. The

27   variability of these time series over 100 bootstrap runs was relatively low, as shown in Fig.

28   S5. In both cities, the three primary sources (HOA, BBOA and RIOA) exhibit a very spiky

29   temporal behavior, while the secondary OOA is characterized by a relatively smooth time

30   series. Figure 4b reports the averaged total OA mass and relative contributions of the OA

31   sources during the measurements in Tartu (top panel) and Tallinn (bottom panel). The

32   reported errors (which correspond to the standard deviation among 100 bootstrap runs) are an

33   indication of the high stability of the solution. Overall, the relative errors vary between 3 %

Atmospheric
Chemistry
and Physics
Discussions

1   and 7 %, except for the RIOA, which shows slightly higher variability during night-time

2   (relative error of 11 % in Tartu and 13 % in Tallinn). Similarly to the total $PM_{2.5}$ mass and as

3   reported in Fig. 4b, neglecting the special events, a strong daily cycle can be observed in the

4   total OA mass, with higher concentrations during day-time (6.0 µg m^{-3} and 6.3 µg m^{-3} in

5   Tartu and Tallinn, respectively) than during night-time (3.4 µg m^{-3} and 4.2 µg m^{-3} in Tartu

6   and Tallinn, respectively). This difference is mostly driven by the increase of primary aerosol

7   emissions (HOA, BBOA and RIOA) during the day. This structure is observed independently

8   of the nature of the measurements (stationary or mobile), indicating that except for the

9   periods where emissions from point sources are sampled, the OA concentrations and sources

10   are rather homogeneous across the sampling area. In terms of relative contribution, OOA is

11   dominant during night-time, explaining on average between 42 and 44 % of the OA mass in

12   Tartu and Tallinn, respectively. HOA and RIOA relative contributions to the total OA are

13   higher during day-time (the relative contribution of HOA increases from about 20 to 32% in

14   Tartu and from 11 to 27% in Tallinn; the relative contribution of RIOA increases from 20 to

15   27 % in Tartu and from 20 to 22 % in Tallinn). BBOA shows similar relative contributions

16   for day- and night-time in Tartu (explaining about 17 % of the OA mass), and slightly lower

17   during the day-time in Tallinn (20 % during day-time and 25 % at night-time).

18   **3.3   Spatial distributions, regional background and urban increments**

19   The average spatial distributions of the four OA sources, SO_4, NO_3, eBC, CO_2 and CO are

20   represented in Fig. 5 and 6 for Tartu and Tallinn, respectively. The spatial distributions of the

21   additionally measured gas and particle components are reported in Fig. S6 and S7. All loops

22   for which all the instruments were running (except CO_2, CO and CH_4 in Tallinn) were

23   averaged on a grid with grid cells of 250 m^2. In order to get comparable distributions from

24   different days of measurements, the 5th percentile (P05) of was subtracted from each single

25   loop for all components. The subtraction of P05 was found to be optimal to decrease the

26   variability among different loops enough to make them comparable. However, as it will be

27   discussed in the following, P05 was not sufficient to capture the regional background

28   concentrations. The color scales in Fig. 5 and 6 represent the averaged enhancement over the

29   background concentrations of each source/species. For a better visualization, the maximum of

30   the color scale was set at the 75th percentile (P75) for SO_4, NO_3, eBC, CO_2 and CO.

31   Moreover, the highest 75th percentile among all OA sources (i.e., 1.2 µg m^{-3} in Tartu and 2.4

32   µg m^{-3} in Tallinn) was used as a maximum for the four OA sources, in order to facilitate the

Atmospheric
Chemistry
and Physics
Discussions

1   comparison among them. Lastly, the sizes of the points represent the number of measurement

2   points that were averaged in each case. Longitude profiles of the enhancements of all

3   considered component were obtained for Tartu by averaging the calculated enhancements in

4   longitude bins (using the same grid of 250 m^2 as above). These results are shown in Fig. 7

5   (averages and standard deviation among all loops), Fig. S8 (median and first and third

6   quartiles) and Fig. S9 (separation of all loops into time-bins of two hours). The longitude

7   profiles in Fig. 7 and Fig. S8 allowed for the calculation of regional background

8   concentrations and urban increments, as defined by Lenschow et al. (2001) and reported in

9   Table 2. The urban concentrations, which are given by the sum of the regional background

10   and the urban increment, represent a mix between urban background and kerbside locations.

11   While the averaged profiles take into account the effects of the measured point sources in the

12   urban area (mostly traffic and residential emissions), the use of the median profiles is

13   expected to exclude these effects, making the results more representative of the urban

14   background concentrations. In the following we will present the results related to the average

15   profiles, followed by the results from the median profiles reported in parenthesis. In all

16   cases, the longitude profiles were fitted using sigmoid functions (black curves). In order to

17   have a constant averaging city area, the fitting limits (indicated with blue and pink arrows)

18   and the x-value of the sigmoid's midpoint (X_0) were determined from the fit of the total $PM_{2.5}$

19   mass (NR-$PM_{2.5}$ plus eBC) and imposed to all other components. In most of the cases the

20   base of the sigmoid functions is slightly above zero. This indicates that the P05 previously

21   subtracted didn't represent the full regional background, which is therefore given by the sum

22   of the average P05 and the base of the sigmoid function. Moreover, the fits on the west side

23   of Tartu show always higher base values than those for the east, indicating the influence of

24   local sources in the considered regional background area west of Tartu. However, these

25   differences between the west and east fits are in most cases rather low, and therefore we use

26   the west-east averages to calculate the urban increments concentrations in Table 2.

27   In Tartu, the three primary OA sources (HOA, BBOA and RIOA) show a clear enhancement

28   in the city center compared to the suburban areas (Fig. 7 and S8). Moreover, different source

29   regions (see Fig. 5a-c) and emission times (see Fig. S9) can be distinguished inside the urban

30   area. For example, maximum HOA concentrations are observed on highly congested roads,

31   especially at sites under stop-and-go conditions, and show a maximum enhancement in the

32   morning and evening traffic rush hours (07:00 to 09:00 and 15:00 to 17:00, LT). The spatial

33   distributions of the eBC, CO_2 and CO (Fig. 5g-i) are consistent with that of HOA, which

1   indicates that these species originate mostly from traffic. BBOA is more strongly enhanced in

2   the residential areas and the maximum enhancement is seen in the evening hours (15:00 to

3   21:00, LT) when domestic heating is more active. RIOA shows enhanced contributions in

4   both, the residential areas (probably related to domestic cooking emissions) and the major

5   roads in the city center (probably related to cooking emissions from restaurants). The

6   maximum enhancement of RIOA is also seen in the evening hours (15:00 to 19:00, LT),

7   during and after the evening maximum of HOA. In contrast, OOA (Fig. 5d) and the other

8   secondary species (SO_4, NO_3, NH_4 and Cl, see Fig. 5e-f and Fig. S6), show very

9   homogeneous spatial distribution over the whole measurement area (as expected from their

10   secondary nature), and no clear dependence on the time of the day can be seen for the OOA

11   (Fig. S8). Although slight enhancements are observed in these components close to

12   residential areas (OOA enhancement of 0.8 $\mu g\ m^{-3}$), these increases are negligible within the

13   measurement and source apportionment uncertainties.

14   As reported in Table 2, the $PM_{2.5}$ mass concentration in Tartu shows an urban increment of

15   6.0 (4.6) $\mu g\ m^{-3}$ over a regional background concentration of 4.0 (3.5) $\mu g\ m^{-3}$. This leads to

16   urban $PM_{2.5}$ mass concentrations of up to 10 (8.1) $\mu g\ m^{-3}$, which represents an increase of a

17   factor 2.5 (2.3) in the particle mass concentration in the urban area compared to the regional

18   background. About half of this enhancement is related to the emissions of eBC, which shows

19   an increase of 3.2 (2.3) $\mu g\ m^{-3}$ over a regional background of 1.1 (0.58) $\mu g\ m^{-3}$. Thus, the

20   urban concentration of eBC is 4.2 (2.9) $\mu g\ m^{-3}$, which represents an enhancement of a factor

21   3.9 (5.0) of eBC in the urban area. The primary OA sources explain great part of the

22   remaining increase in the $PM_{2.5}$ mass: HOA is increased by a factor 3.6 (3.0) in the urban

23   area and has contribution of 1.7 (1.0) $\mu g\ m^{-3}$ to the urban concentration; RIOA is enhanced

24   by a factor 2.0 (2.3), contributing with 1.7 (1.0) $\mu g\ m^{-3}$ to the urban concentration; and

25   BBOA is enhanced by a factor 3.1 (2.4) and contributes with 1.0 (0.52) $\mu g\ m^{-3}$ to the urban

26   concentrations. On the other hand, OOA and the inorganic species (SO_4, NO_3, NH_4 and Cl)

27   show very low increases in the urban area, resulting in a total urban increment below 0.21 μg

28   m^{-3} (average and median). In the gas-phase, CO_2 shows an increase of 8.3 (5.3) ppm over a

29   regional background of 403.5 ppm (both average and median); CO is increased by 0.15 (0.11)

30   ppm over a regional background of 0.16 (0.14) ppm, which represents an increase of a factor

31   1.9 (1.7); while CH_4 shows very similar concentrations inside and outside the city, with

32   average (and median) regional background of 1.90 ppm and urban concentrations of 1.91

33   ppm.

1   Similar results were obtained for Tallinn (see Fig. 6 and Fig. S7). However, given the larger

2   extension of this city, it wasn't possible to include a real regional background site in the

3   route. Therefore, the longitude profiles and urban increments couldn't be properly explored

4   for Tallinn. However, different source regions can still be distinguished within the examined

5   area. Thus, the spatial distribution of HOA (Fig. 6a) is in agreement with those of eBC, CO_2

6   and CO (Fig. 6g-i) and shows substantial increases in areas with high traffic and on major

7   streets in the city center with significant stop-and-go conditions. BBOA (Fig. 6b) has higher

8   contributions in the two residential areas, while compared to Tartu, in Tallinn the spatial

9   distribution of RIOA (Fig. 6c) is more homogeneous, with only slight enhancements in the

10   residential area and in the city center. Finally, OOA (Fig. 6d) exhibits a small enhancement in

11   the city center area, which again coincides with small increases in the secondary inorganic

12   species concentrations (see Fig. 6e-f and Fig. S7) that are insignificant within the

13   measurement and source apportionment uncertainties. Enhanced SO_4 levels are also found in

14   the northern part of the route, likely from local ship emissions (Lack et al., 2009).

15   **3.4   Special events: transport and accumulation of pollutants**

16   Enhanced concentrations of secondary species including OOA, SO_4, NO_3 and NH_4 were

17   measured during the first measurement day in Tartu (see Fig. 2a and Fig. 4a). The analysis of

18   the 24-hour back-trajectories reported in Fig. 8a indicates that these mostly secondary

19   components were probably transported from continental Europe, in particular from northern

20   Germany. The later decrease in the concentrations of these species coincides with clean air

21   masses originating from the Northern Atlantic at higher altitudes above ground level. As

22   reported in Fig. 8b, during this transport event the average $PM_{2.5}$ mass concentration

23   increased to 28.3 μg m^{-3} (compared to average concentrations of 11.0 μg m^{-3} measured

24   during day-time and 6.5 μg m^{-3} during night-time). This increase in mass is mostly related to

25   the increased concentrations of the secondary components, especially of NO_3 and OOA.

26   Accordingly, the relative contributions of the inorganic species to the total $NR-PM_{2.5}$

27   increased to over 44 % during the transport event (compared to 12 % for day-time and around

28   28 % for night-time averages) and the relative contribution of the OOA to total OA increased

29   to 56 % (compared to 25 % for day-time and 42 % for night-time averages). It is worth to

30   note that source separation is more uncertain during the transport event due to lower statistics

31   and increased mixing (if the transported air contains multiple sources). This is especially the

Atmospheric
Chemistry
and Physics
Discussions

Open Access

EGU

1   case for RIOA, which has a relative error of 41 % (estimated by the bootstrapping procedure)

2   during the transport event.

3   During the nights of 28 and 29 March, very high concentrations of organics (exceeding 200

4    $\mu g \ m^{-3}$), eBC (above 15 $\mu g \ m^{-3}$) and CO_2 (up to 500 ppm) were measured in Tallinn, as

5   shown in Fig. 9a. Relatively short back-trajectories originating from the Baltic Sea (North-

6   West and West from the sampling site) and at high altitudes were obtained for these periods

7   (not reported). Moreover, as shown in Fig. 9a, during such accumulation events wind speed

8   was close to zero and a strong near-ground temperature inversion (i.e. a positive temperature

9   difference between the ground and 22 m above ground level (AGL)) was observed. Under

10   such conditions, the vertical mixing is suppressed and the local pollutants are trapped at the

11   surface. As reported in Fig. 9b, during the accumulation periods the average $PM_{2.5}$ mass

12   increased up to 41.7 $\mu g \ m^{-3}$, with OA explaining 73 % of the total mass. This increase was

13   mostly related to the increase of the primary aerosols, mainly HOA and BBOA, which

14   explained 33 and 37 % of the OA mass, respectively.

15

16   **4   Conclusions**

17   Mobile measurements allowed for the study of the spatial distributions of major gas- and

18   particle-phase pollutants in two urban areas in Estonia, permitting the identification of

19   particular source areas and the determination of regional background concentrations and

20   urban increments for the individual components/sources. A comprehensive set of instruments

21   including a HR-ToF-AMS (with a newly developed inlet to measure the NR-$PM_{2.5}$ fraction),

22   a 7-wavelength Aethalometer and several gas-phase monitors were deployed in the mobile

23   laboratory to retrieve a detailed chemical characterization of the $PM_{2.5}$ fraction and the

24   concentrations of several trace gases with high time resolution.

25   The measurements were performed in March 2013 in the two major cities of Estonia (Tallinn

26   and Tartu) and no major differences were found in the chemical composition at the two sites.

27   Higher mass concentrations were always measured during day-time, when point sources were

28   sampled during mobile measurements. Under regular meteorological conditions, OA

29   represented the largest mass fraction (on average 52.2 % to 60.1 % of $PM_{2.5}$), while the

30   relative contribution of the inorganic species (mostly SO_4, NO_3 and NH_4) strongly increased

31   during the transport of polluted air masses from northern Germany. Four sources of OA were

32   identified by means of PMF: three primary sources (HOA, BBOA and RIOA) and a

Atmospheric
Chemistry
and Physics
Discussions

1   secondary OA (OOA). Although the RIOA is thought to be dominated by cooking emissions,

2   contributions from other residential emissions to this factor cannot be excluded. For example,

3   waste burning is known to be a common process in some cities in Estonia (Maasikmets et al.,

4   2015). However, to properly separate the contribution of waste burning from other co-

5   emitting sources, laboratory studies of direct emissions need to be performed in the future.

6   While OOA dominated the OA mass during night-time (on average 42.3 % in Tartu and 43.8

7   % in Tallinn), the primary sources explained the major fraction of OA during day-time (75.2

8   % in Tartu and 68.3 % in Tallinn, with similar contributions from the three sources). During

9   the period with transport of polluted air masses aforementioned, the OOA relative

10   contribution was enhanced. In contrast, HOA, RIOA and BBOA were strongly enhanced

11   during periods characterized by temperature inversions, which induced the accumulation of

12   locally emitted primary pollutants (primary OA and eBC).

13   Different source regions were identified inside the two urban areas. All traffic related

14   pollutants (including HOA, eBC, CO_2 and CO) where strongly enhanced on the major city

15   roads, especially in areas with stop-and-go conditions during the morning and evening rush

16   hours. BBOA showed a clear increase in the residential areas during the evening hours (due

17   to domestic heating), while RIOA (believed to be strongly influenced by cooking emissions)

18   was enhanced in both, the city center (from restaurant cooking emissions) and in the

19   residential areas (from domestic cooking). In contrast, the secondary components (including

20   OOA, SO_4, NO_3, NH_4 and Cl) had very homogeneous spatial distributions, with no clear

21   enhancement in the urban areas (within the measurement uncertainties) or at certain times of

22   the day. For Tartu, regional background concentrations and urban increments of all measured

23   components/sources were also determined. On average, the $PM_{2.5}$ mass had an enhancement

24   inside the city of 6.0 µg m^{-3} over the regional background concentration of 4.0 µg m^{-3}. This

25   urban increment was strongly related to the enhancement of eBC (3.2 µg m^{-3}) and the

26   primary OA sources (on average 1.2 µg m^{-3} from HOA, 0.67 µg m^{-3} from BBOA and 0.72 µg

27   m^{-3} from RIOA), while the secondary components (OOA, SO_4, NO_3, NH_4 and Cl) didn't

28   contribute to a substantial enhancement. Moreover, the good correlation found between eBC

29   with HOA indicates that up to 74 % of the enhancement in the $PM_{2.5}$ is related to traffic

30   emissions in the urban area. CO_2 and CO, which were also found to be strongly correlated

31   with HOA, had an average urban increment of 8.3 and 0.15 ppm over regional background

32   concentrations of 403.5 and 0.15 ppm, respectively.

Atmospheric
Chemistry
and Physics
Discussions

Open Access

EGU

1 Our results show that mobile measurements are a very powerful technique for spatial

2 characterization of the major pollutants in urban areas. The methodology presented in this

3 work can be generalized to other cities, in order to determine the influence of human activity

4 on the particle sources and levels in different areas of a city and the related health effects.

5

6 **Acknowledgments**

17

18

19

20

21

22

23

24

Atmospheric
Chemistry
and Physics
Discussions

Open Access

EGU

1 **References**

2   Alfarra, M. R., Prévôt, A. S. H., Szidat, S., Sandradewi, J., Weimer, S., Lanz, V. A.,

3   Schreiber, D., Mohr, M., and Baltensperger, U.: Identification of the mass spectral signature

4   of organic aerosols from wood burning emissions, Environ. Sci. Technol., 41, 5770–5777,

5   2007.

6   Allan, J. D., Delia, A. E., Coe, H., Bower, K. N., Alfarra, M. R., Jimenez, J. L., Middlebrook,

7   A. M., Drewnick, F., Onasch, T. B., Canagaratna, M. R., Jayne, J. T., and Worsnopf, D. R.: A

8   generalized method for the extraction of chemically resolved mass spectra from Aerodyne

9   aerosol mass spectrometer data, J. Aerosol Sci., 35, 909–922, 2004.

10   Ångström, A.: On the atmospheric transmission of sun radiation and on dust in the air, Geogr.

11   Ann., 11, 156–166, 1929.

12   Baker, J.: A cluster analysis of long range air transport pathways and associated pollutant

13   concentrations within the UK, Atmos. Environ., 44, 563–571, 2010.

14   Beekmann, M., Prévôt, A. S. H., Drewnick, F., Sciare, J., Pandis, S. N., Denier van der Gon,

15   H. A. C., Crippa, M., Freutel, F., Poulain, L., Ghersi, V., Rodriguez, E., Beirle, S., Zotter, P.,

16   von der Weiden-Reinmüller, S.-L., Bressi, M., Fountoukis, C., Petetin, H., Szidat, S., Schn,

17   J., Borbon, A, Gros, V., Marchand, N., Jaffrezo, J. L., Schwarzenboeck, A., Colomb, A.,

18   Wiedensohler, A., Borrmann, S., Lawrence, M., Baklanov, A., and Baltensperger, U.: In-situ,

19   satellite measurement and model evidence for a dominant regional contribution to fine

20   particulate matter levels in the Paris Megacity, Atmos. Chem. Phys., 15, 9577-9591, 2015.

21   Bukowiecki, N., Dommen, J., Prévôt, A. S. H., Richter, R., Weingartner, E., and

22   Baltensperger, U.: A mobile pollutant measurement laboratory: measuring gas phase and

23   aerosol ambient concentrations with high spatial and temporal resolution, Atmos. Environ.,

24   36, 5569–5579, 2002.

25   Canonaco, F., Crippa, M., Slowik, J. G., Baltensperger, U., and Prévôt, A. S. H.: SoFi, an

26   IGOR-based interface for the efficient use of the generalized multilinear engine (ME-2) for

27   the source apportionment: ME-2 application to aerosol mass spectrometer data, Atmos. Meas.

28   Tech., 6, 3649–3661, 2013.

29   Carbone, C., Decesari, S., Mircea, M., Giulianelli, L., Finessi, E., Rinaldi, M., Fuzzi, S.,

30   Marinoni, A., Duchi, R., Perrino, C., Sargolini, T., Vardè, M., Sprovieri, F., Gobbi, G. P.,

31   Angelini, F., and Facchini, M. C.: Size-resolved aerosol chemical composition over the

Atmospheric
Chemistry
and Physics
Discussions

1   Italian Peninsula during typical summer and winter conditions, Atmos. Environ., 44, 5269–

2   5278, 2010.

3   Crippa, M., DeCarlo, P. F., Slowik, J. G., Mohr, C., Heringa, M. F., Chirico, R., Poulain, L.,

4   Freutel, F., Sciare, J., Cozic, J., Di Marco, C. F., Elsasser, M., Nicolas, J. B., Marchand, N.,

5   Abidi, E., Wiedensohler, A., Drewnick, F., Schneider, J., Borrmann, S., Nemitz, E.,

6   Zimmermann, R., Jaffrezo, J.-L., Prévôt, A. S. H., and Baltensperger, U.: Wintertime aerosol

7   chemical composition and source apportionment of the organic fraction in the metropolitan

8   area of Paris, Atmos. Chem. Phys., 13, 961-981, 2013.

9   Crippa, M., El Haddad, I., Slowik, J. G., DeCarlo, P. F., Mohr, C., Heringa, M. F., Chirico,

10   R., Marchand, N., Sciare, J., Baltensperger, U., and Prévôt A. S. H.: Identification of marine

11   and continental aerosol sources in Paris using high resolution aerosol mass spectrometry, J.

12   Geophys. Res., 118, 1950–1963, 2013.

13   DeCarlo, P. F., Kimmel, J. R., Trimborn, A., Northway, M. J., Jayne, J. T., Aiken, A. C.,

14   Gonin, M., Fuhrer, K., Horvath, T., Docherty, K. S., Worsnop, D. R., and Jimenez, J. L.:

15   Field-deployable, high-resolution, time-of-flight aerosol mass spectrometer, Anal. Chem., 78,

16   8281–8289, 2006.

17   Di Gilioa, A., de Gennaroa, G., Dambruosoa, P., and Ventrellaa, G.: An integrated approach

18   using high time-resolved tools to study the origin of aerosols, Sci. Total Environ., 530–531,

19   28–37, 2015.

20   Dockery, D. W., Pope, C. A., Xu, X., Spengler, J. D., Ware, J. H., Fay, M. E., Ferris, B. G. Jr,

21   and Speizer, F. E.: An association between air pollution and mortality in six U.S. cities, N.

22   Engl. J. Med., 329, 1753–1759, 1993.

23   Drinovec, L., Močnik, G., Zotter, P., Prévôt, A. S. H., Ruckstuhl, C., Coz, E., Rupakheti, M.,

24   Sciare, J., Müller, T., Wiedensohler, A., and Hansen, A. D. A.: The "dual-spot"

25   Aethalometer: an improved measurement of aerosol black carbon with real-time loading

26   compensation, Atmos. Meas. Tech., 8, 43–55, 2015.

27   El Haddad, I., D'Anna, B., Temime-Roussel, B., Nicolas, M., Boreave, A., Favez, O., Voisin,

28   D., Sciare, J., George, C., Jaffrezo, J.-L., Wortham, H., and Marchand, N.: Towards a better

29   understanding of the origins, chemical composition and aging of oxygenated organic

30   aerosols: case study of a Mediterranean industrialized environment, Marseille, Atmos. Chem.

31   Phys., 13, 7875-7894, doi:10.5194/acp-13-7875-2013, 2013.

Atmospheric
Chemistry
and Physics
Discussions

Open Access

EGU

1 Elser, M., Huang, R.-J., Wolf, R., Slowik, J. G., Wang, Q.-Y., Canonaco, F., Li, G. H.,
2 Bozzetti, C., Daellenbach, K. R., Huang, Y., Zhang, R.-J., Li, Z.-Q., Cao, J. J., Baltensperger,
3 U., El-Haddad, I., and Prévôt, A. S. H.: New insights into $PM_{2.5}$ chemical composition and
4 sources in two major cities in China during extreme haze events using aerosol mass
5 spectrometry, Atmos. Chem. Phys. Discuss., 15, 30127–30174, 2015.

6 Gao, M., Guttikunda, S. K., Carmichael, G. R., Wang, Y., Liu, Z., Stanier, C. O., Saide, P. E.,
7 and Yu, M.: Health impacts and economic losses assessment of the 2013 severe haze event in
8 Beijing area, Sci. Total Environ., 511, 553–561, 2015.

9 Hu, D. and Jiang, J.: PM2.5 pollution and risk for lung cancer: A rising issue in China, J.
10 Environ. Prot., 5, 731–738, 2014.

11 Jimenez, J. L., Canagaratna, M. R., Donahue, N. M., Prévôt, A. S. H., Zhang, Q., Kroll, J. H.,
12 DeCarlo, P. F., Allan, J. D., Coe, H., Ng, N. L., Aiken, A. C., Docherty, K. S., Ulbrich, I. M.,
13 Grieshop, A. P., Robinson, A. L., Duplissy, J., Smith, J. D., Wilson, K. R., Lanz, V. A.,
14 Hueglin, C., Sun, Y. L., Tian, J., Laaksonen, A., Raatikainen, T., Rautiainen, J., Vaattovaara,
15 P., Ehn, M., Kulmala, M., Tomlinson, J. M., Collins, D. R., Cubison, M. J., Dunlea, E. J.,
16 Huffman, J. A., Onasch, T. B., Alfarra, M. R., Williams, P. I., Bower, K., Kondo, Y.,
17 Schneider, J., Drewnick, F., Borrmann, S., Weimer, S., Demerjian, K., Salcedo, D., Cottrell,
18 L., Griffin, R., Takami, A., Miyoshi, T., Hatakeyama, S., Shimono, A., Sun, J. Y., Zhang, Y.
19 M., Dzepina, K., Kimmel, J. R., Sueper, D., Jayne, J. T., Herndon, S. C., Trimborn, A. M.,
20 Williams, L. R., Wood, E. C., Middlebrook, A. M., Kolb, C. E., Baltensperger, U., and
21 Worsnop, D. R.: Evolution of organic aerosols in the atmosphere, Science, 326, 1525–1529,
22 2009.

23 Kwak, J. H., Kim, H. S., Lee, J. H., and Lee, S. H.: On-road chasing measurement of exhaust
24 of particle emissions from diesel, CNG LPG and DME-fueled vehicles using a mobile
25 emission laboratory, Int. J. Vehicle Des., 15, 543–551, 2014.

26 Kyung Hwan, K., Daekwang, W., Seung-Bok, L., and Gwi-Nam, B.: On-road measurements
27 of ultrafine particles and associated air pollutants in a densely populated area of Seoul, Korea,
28 Aerosol Air Qual. Res., 15, 142–153, 2015.

29 Lack, D. A., Corbett, J. J., Onasch, T., Lerner, B., Massoli, P., Quinn, P. K., Bates, T. S.,
30 Covert, D. S., Coffman, D., Sierau, B., Herndon, S., Allan, J., Baynard, T., Lovejoy, E.,
31 Ravishankara, A. R., and Williams, E.: Particulate emissions from commercial shipping:

Atmospheric
Chemistry
and Physics
Discussions

1   Chemical, physical, and optical properties, J. Geophys. Res., 114, D00F04, doi:
2   10.1029/2008JD011300, 2009.

3   Laden, F., Schwartz, J., Speizer, F. E., and Dockery, D. W.: Reduction in fine particulate air
4   pollution and mortality: Extended follow-up of the Harvard Six Cities study, Am. J. Respir.
5   Crit. Care. Med., 173, 667–672, 2006.

6   Lenschow, P., Abraham, H. J., Kutzner, K., Lutz, M., Preuß, J. D., and Reichenbächer, W.:
7   Some ideas about the sources of PM10, Atmos. Environ., 35, Supplement 1, S23–S33, 2001.

8   Maasikmets, M., Kupri, H-L., Teinemaa, E., Vainumäe, K., Arumäe, T., and Kimmel, V.:
9   ACSM study to assess possible municipal solid waste burning in household stoves. Poster
10 presented at: European Aerosol Conference 2015, Milan (Italy), September 6-11, 2015.

11 Middlebrook, A. M., Bahreini, R., Jimenez, J. L., and Canagaratna, M. R.: Evaluation of
12 composition-dependent collection efficiencies for the Aerodyne aerosol mass spectrometer
13 using field data, Aerosol Sci. Technol., 46, 258–271, 2012.

14 Mohr, C., Richter, R., DeCarlo, P. F., Prévôt, A. S. H., and Baltensperger, U.: Spatial
15 variation of chemical composition and sources of submicron aerosol in Zurich during
16 wintertime using mobile aerosol mass spectrometer data, Atmos. Chem. Phys., 11, 7465–
17 7482, 2011.

18 Mohr, C., DeCarlo, P. F., Heringa, M. F., Chirico, R., Slowik, J. G., Richter, R., Reche, C.,
19 Alastuey, A., Querol, X., Seco, R., Peñuelas, J., Jiménez, J. L., Crippa, M., Zimmermann, R.,
20 Baltensperger, U. and Prévôt, A. S. H.: Identification and quantification of organic aerosol
21 from cooking and other sources in Barcelona using aerosol mass spectrometer data, Atmos.
22 Chem. Phys., 12, 1649–1665, 2012.

23 Mohr, C., DeCarlo, P. F., Heringa, M. F., Chirico, R., Richter, R., Crippa, M., Querol, X.,
24 Baltensperger, U., and Prévôt, A. S. H.: Spatial variation of aerosol chemical composition
25 and organic components identified by positive matrix factorization in the Barcelona region,
26 Environ. Sci. Technol., 49, 10421–10430, 2015.

27 Myhre, G., Shindell, D., Bréon, F.-M., Collins, W., Fuglestvedt, J., Huang, J., Koch, D.,
28 Lamarque, J.-F., Lee, D., Mendoza, B., Nakajima, T., Robock, A., Stephens, G., Takemura,
29 T., and Zhang, H.: Anthropogenic and Natural Radiative Forcing. In: Climate Change 2013:
30 The Physical Science Basis. Contribution of Working Group I to the Fifth Assessment Report
31 of the Intergovernmental Panel on Climate Change [Stocker, T.F., Qin, D., Plattner, G.-K.,

Atmospheric
Chemistry
and Physics
Discussions

Open Access

EGU

1   Tignor, M., Allen, S. K., Boschung, J., Nauels, A., Xia, Y., Bex, V., and Midgley, P. M.

2   (eds.)]. Cambridge University Press, Cambridge, United Kingdom and New York, NY, USA,

3   2013.

4   Ng, N. L., Canagaratna, M. R., Jimenez, J. L., Zhang, Q., Ulbrich, I. M., and Worsnop, D. R.:

5   Real-time methods for estimating organic component mass concentrations from aerosol mass

6   spectrometer data, Environ. Sci. Technol., 45, 910–916, 2011.

7   Niemi, J. V., Saarikoski, S., Aurela, M., Tervahattu, H., Hillamo, R., Westphal, D. L.,

8   Aarnio, P., Koskentalo, T., Makkonen, U.,Vehkamaki, H., and Kulmala, M.: Long-range

9   transport episodes of fine particles in southern Finland during 1999–2007, Atmos. Environ.,

10   43, 1255–1264, 2009.

11   Orru, H., Maasikmets, M., Lai, T., Tamm, T., Kaasik, M., Kimmel, V., Orru, K., Merisalu,

12   E., and Forsberg, B.: Health impacts of particulate matter in five major Estonian towns: main

13   sources of exposure and local differences, Air Qual. Atmos. Health, 4, 247–258, 2011.

14   Paatero, P. and Tapper, U.: Positive matrix factorization: a non-negative factor model with

15   optimal utilization of error estimates of data values, Environmetrics, 5, 111–126, 1994.

16   Paatero, P.: Least squares formulation of robust non-negative factor analysis, Chemom. Intell.

17   Lab. Syst., 37, 23–35, 1997.

18   Paatero, P. and Hopke, P. K.: Discarding or downweighting high-noise variables in factor

19   analytic models, Anal. Chim. Acta, 490, 277–289, 2003.

20   Paatero, P., Eberly, S., Brown, S. G., and Norris G. A.: Methods for estimating uncertainty in

21   factor analytic solutions, Atmos. Meas. Tech., 7, 781–797, 2014.

22   Pirjola, L., Parviainen, H., Hussein, T., Valli, A., Hämeri, K., Aalto, P., Virtanen, A.,

23   Keskinen, J., Pakkanen, T. A., Mäkelä, T., and Hillamo, R. E.: "Sniffer" - a novel tool for

24   chasing vehicles and measuring traffic pollutants. Atmos. Environ., 38, 3625–3635, 2004.

25   Pirjola, L., Paasonen, P., Pfeiffer, D., Hussein, T., Hämeri, K., Koskentalo, T., Virtanen, A.,

26   Rönkkö, T., Keskinen, J., Pakkanen, T. A., and Hillamo, R. E.: Dispersion of particles and

27   trace gases nearby a city highway: mobile laboratory measurements in Finland, Atmos.

28   Environ., 40, 867–879, 2006.

29   Pirjola, L., Lähde, T., Niemi, J. V., Kousa, A., Rönkkö, T., Karjalainen, P., Keskinen, J.,

30   Frey, A.,and Hillamo, R. E.: Spatial and temporal characterization of traffic emission in

31   urban microenvironments with a mobile laboratory, Atmos. Environ., 63, 156–167, 2012.

Atmospheric
Chemistry
and Physics
Discussions

1   Pirjola, L., Virkkula, A., Petaja, T., Levula, J., Kukkonen, J., and Kulmala, M.: Mobile
2   ground-based measurements of aerosol and trace gases during a prescribed burning
3   experiment in boreal forest in Finland, Boreal Environ. Res., 20, 105–119, 2015.

4   Pope, C. A. and Dockery, D. W.: Health effects of fine particulate air pollution: lines that
5   connect, J. Air Waste Manag. Assoc., 56, 709–742, 2006.

6   Putaud, J. P., Raes, F., Van Dingenen, R., Brüggemann, E., Facchini, M. C., Decesari, S.,
7   Fuzzi, S., Gehrig, R., Hüglin, C., Laj, P., Lorbeer, G., Maenhaut, W., Mihalopoulos, N.,
8   Müller, K., Querol, X., Rodriguez, S., Schneider, J., Spindler, G., ten Brink, H., Tørseth, K.,
9   and Wiedensohler, A.: A European aerosol phenomenology - 2: chemical characteristics of
10 particulate matter at kerbside, urban, rural and background sites in Europe, Atmos. Environ.,
11 38, 2579–2595, 2004.

12 Putaud, J.-P., Van Dingenen, R., Alastuey, A., Bauer, H., Birmili, W., Cyrys, J., Flentje, H.,
13 Fuzzi, S., Gehrig, R., Hansson, H. C., Harrison, R. M., Herrmann, H., Hitzenberger, R.,
14 Hüglin, C., Jones, A. M., Kasper-Giebl, A., Kiss, G., Kousam, A., Kuhlbusch, T. A. J.,
15 Löschau, G., Maenhaut, W., Molnar, A., Moreno, T., Pekkanen, J., Perrino, C., Pitz, M.,
16 Puxbaum, H., Querol, X., Rodriguez, S., Salma, I., Schwarz, J., Smolik, J., Schneider, J.,
17 Spindler, G., ten Brink, H., Tursic, J., Viana, M., Wiedensohler, A., and Raes, F.: A European
18 aerosol phenomenology - 3: Physical and chemical characteristics of particulate matter from
19 60 rural, urban, and kerbside sites across Europe, Atmos. Environ., 44, 1308–1320, 2010.

20 Ramanathan, V., Crutzen, P. J., Kiehl, J. T., and Rosenfeld, D.: Aerosols, climate, and the
21 hydrological cycle, Science, 294, 2119–2124, 2001.

22 Salvador, P., Artinano, B., Molero, F., Viana, M., Pey, J., Alastuey, A., and Querol, X.:
23 African dust contribution to ambient aerosol levels across central Spain: Characterization of
24 long-range transport episodes of desert dust, Atmos. Res., 127, 117–129, 2013.

25 Sandradewi, J., Prévôt, A. S. H., Szidat, S., Perron, N., Alfarra, M. R., Lanz, V. A.,
26 Weingartner, E., and Baltensperger, U.: Using aerosol light absorption measurements for the
27 quantitative determination of wood burning and traffic emission contributions to particulate
28 matter, Environ. Sci. Technol., 42, 3316–3323, 2008.

29 Squizzato, S., Masiol, M., Innocente, E., Pecorari, E., Rampazzo, G., and Pavoni, B.: A
30 procedure to assess local and long-range transport contributions to PM2.5 and secondary
31 inorganic aerosol, J. Aerosol Sci., 46, 64–76, 2012.

Atmospheric
Chemistry
and Physics
Discussions

1   Statistical database, Statistics Estonia: http://pub.stat.ee, last access: 09 November 2015.

2   Sun, Y. L., Zhang, Q., Schwab, J. J., Demerjian, K. L., Chen, W. N., Bae, M.-S., Hung, H.-
3   M, Hogrefe, O., Frank, B., Rattigan, O.V., and Lin, Y.-C.: Characterization of the sources
4   and processes of organic and inorganic aerosols in New York City with a high-resolution
5   time-of-flight aerosol mass spectrometer, Atmos. Chem. Phys., 11, 1581–1602, 2011.

6   Ulbrich, I. M., Canagaratna, M. R., Zhang, Q., Worsnop, D. R., and Jimenez, J. L.:
7   Interpretation of organic components from positive matrix factorization of aerosol mass
8   spectrometric data, Atmos. Chem. Phys., 9, 2891–2918, 2009.

9   Ulevicius, V., Byčenkienė, S., Bozzetti, C., Vlachou, A., Plauškaitė, K., Mordas, G.,
10   Dudoitis, V., Abbaszade, G., Remeikis, V., Garbaras, A., Masalaite, A., Blees, J., Fröhlich,
11   R., Dällenbach, K. R., Canonaco, F., Slowik, J. G., Dommen, J., Zimmermann, R., Schnelle-
12   Kreis, J., Salazar, G. A., Agrios, K., Szidat, S., El Haddad, I., and Prévôt, A. S. H.: Fossil and
13   non-fossil source contributions to atmospheric carbonaceous aerosols during extreme spring
14   grassland fires in Eastern Europe, Atmos. Chem. Phys. Discuss., 15, 26315–26355, 2015.

15   Urb, G., Teinemaa, E., Kettrup A., Gebefügi, I., Laja, M., Reinik, J., Tamm, E., Kirso, U.:
16   Atmospheric pollution in Tallinn, levels of priority pollutants, Proc. Estonian Acad. Sci.
17   Chem., 54, 123–133, 2005.

18   Von der Weiden-Reinmueller, S.-L, Drewnick, F., Crippa, M., Prévôt, A. S. H., Meleux, F.,
19   Baltensperger, U., Beekmann, M., and Borrmann, S.: Application of mobile aerosol and trace
20   gas measurements for the investigation of megacity air pollution emissions: the Paris
21   metropolitan area, Atmos. Meas. Tech., 7, 279–299, 2014a.

22   Von der Weiden-Reinmueller, S.-L., Drewnick, F., Zhang, Q. J., Freutel, F., Beekmann, M.,
23   and Borrmann, S.: Megacity emission plume characteristics in summer and winter
24   investigated by mobile aerosol and trace gas measurements: the Paris metropolitan area,
25   Atmos. Chem. Phys., 14, 12931–12950, 2014b.

26   Williams, L. R., Gonzalez, L. A., Peck, J., Trimborn, D., McInnis, J., Farrar, M. R., Moore,
27   K. D., Jayne, J. T., Robinson, W. A., Lewis, D. K., Onasch, T. B., Canagaratna, M. R.,
28   Trimborn, A., Timko, M. T., Magoon, G., Deng, R., Tang, D., de la Rosa Blanco, E., Prévôt,
29   A. S. H., Smith, K. A., and Worsnop, D. R.: Characterization of an aerodynamic lens for
30   transmitting particles greater than 1 micrometer in diameter into the Aerodyne aerosol mass
31   spectrometer, Atmos. Meas. Tech,, 6, 3271–3280, 2013.

Atmospheric
Chemistry
and Physics
Discussions

Open Access

1   Wolf, R., El Haddad, I., Crippa, M., Decesari, S., Slowik, J. G., Poulain, L., Gilardoni, S.,

2   Rinaldi, M., Carbone, S., Canonaco, F., Huang, R.-J., Baltensperger, U., and Prévôt, A. S. H.:

3   Marine and urban influences on summertime PM2.5 aerosol in the Po basin using mobile

4   measurements, Atmos. Environ., 120, 447–454, 2015.

5   Zotter, P., Herich, H., Gysel, M., El-Haddad, I., Zhang, Y. L., Močnik, G., Hüglin, C.,

6   Baltensperger, U., Szidat, S., and Prévôt, A. S. H.: Evaluation of the absorption Ångström

7   exponents for traffic and wood burning in the Aethalometer based source apportionment

8   using radiocarbon measurements of ambient aerosol, In preparation.

9

10

11

12

13

14

15

16

17

18

19

20

21

22

23

24

25

26

27

Atmospheric
Chemistry
and Physics
Discussions

1   Table 1: Instrument list, measured components and time resolution of each measurement.

2

	Instrument list	Measured components	Time resolution
Aerosols	**HR-ToF-AMS**	*Size resolved chemical composition of NR-PM2.5*	*25 sec*
	Aethalometer	*BC (7λ)*	*1 sec*
Gas	**CO₂ Picarro**	*CO_2, CO, CH_4, H_2O*	*1 sec*
	CO₂ Licor	*CO_2, H_2O*	*1 sec*
Others	**GPS, Temperature, Relative humidity & Solar radiation**		*2 sec*

Atmospheric
Chemistry
and Physics
Discussions

1 Table 2: Results obtained from the average (A) and median (B) longitude profiles for each

2 measured component/source. P05 represents the averaged 5th percentile subtracted for the

3 calculation of the enhancements; base and increment values were obtained from the sigmoid

4 fits; the regional background is given as the sum of P05 and the average base value; urban

5 concentrations are the sum of the regional background and the average urban increment; the

6 factor increase represents the ratio between the urban and the regional backgrounds.

7 **(A) Average longitude profiles:**

	P05[(1)]	Base			Urban increment			Regional background	Urban concentration	Factor increase
		West	East	Average	West	East	Average			
PM$_{2.5}$ (µg m^{-3})	1.8	2.6	1.8	2.2	5.6	6.3	6.0	**4.0**	**10.0**	**2.5**
HOA (µg m-3)	0.18	0.34	0.24	0.29	1.2	1.3	1.2	**0.47**	**1.7**	**3.6**
BBOA$^{(2)}$ (µg m-3)	0.11	0.24 (0.16)	0.19	0.21	0.60 (0.64)	0.75	0.67	**0.32**	**1.0**	**3.1**
RIOA (µg m-3)	0.27	0.44	-0.30	0.44	0.72	1.9	0.72	**0.71**	**1.4**	**2.0**
OOA (µg m-3)	0.44	0.42	0.32	0.37	0.024	0.11	0.069	**0.81**	**0.87**	**1.1**
SO$_4$ (µg m-3)	0.29	0.075	0.055	0.065	0.032	0.051	0.042	**0.35**	**0.39**	**1.1**
NO$_3$ (µg m-3)	0.095	0.075	0.076	0.075	0.042	0.038	0.040	**0.17**	**0.21**	**1.2**
NH$_4$ (µg m-3)	0.079	0.032	0.028	0.030	0.012	0.016	0.014	**0.11**	**0.12**	**1.1**
Cl (µg m-3)	0.012	0.036	0.035	0.035	0.022	0.022	0.022	**0.047**	**0.069**	**1.5**
eBC (µg m-3)	0.34	0.96	0.54	0.75	3.0	3.3	3.2	**1.1**	**4.2**	**3.9**
CO$_2$ (ppm)	403.0	0.99	0.04	0.52	7.8	8.9	8.3	**403.5**	**411.9**	**1.0**
CO (ppm)	0.14	0.028	0.012	0.020	0.14	0.15	0.15	**0.16**	**0.31**	**1.9**
CH$_4^{(3)}$ (ppm)	1.90	0.0060 (0.0052)	<0.001	0.0012	0.0047 (0.0064)	0.012	0.0083	**1.90**	**1.91**	**1.0**

(B) Median longitude profiles:

	P05[(1)]	Base			Urban increment			Regional background	Urban concentration	Factor increase
		West	East	Average	West	East	Average			
PM$_{2.5}$ (µg m^{-3})	1.8	1.8	1.6	1.7	4.6	4.6	4.6	**3.5**	**8.1**	**2.3**
HOA (µg m-3)	0.18	0.16	0.13	0.14	0.66	0.66	0.66	**0.33**	**1.0**	**3.0**
BBOA (µg m^{-3})	0.11	0.088	0.12	0.11	0.35	0.27	0.31	**0.22**	**0.52**	**2.4**
RIOA (µg m-3)	0.27	0.20	0.15	0.17	0.58	0.60	0.59	**0.45**	**1.0**	**2.3**
OOA (µg m-3)	0.44	0.28	0.26	0.27	0.084	0.096	0.090	**0.71**	**0.80**	**1.1**
SO$_4$ (µg m-3)	0.29	0.064	0.053	0.059	0.029	0.039	0.034	**0.35**	**0.38**	**1.1**
NO$_3$ (µg m-3)	0.095	0.043	0.053	0.048	0.056	0.039	0.047	**0.14**	**0.19**	**1.3**
NH$_4$ (µg m-3)	0.079	0.028	0.026	0.027	0.0094	0.011	0.010	**0.11**	**0.12**	**1.1**
Cl (µg m-3)	0.012	0.022	0.025	0.024	0.024	0.019	0.021	**0.035**	**0.06**	**1.6**
eBC (µg m-3)	0.34	0.45	0.027	0.24	2.0	2.5	2.3	**0.58**	**2.9**	**5.0**
CO$_2$ (ppm)	403.0	0.95	0.051	0.50	5.0	5.6	5.3	**403.5**	**408.8**	**1.0**
CO (ppm)	0.14	0.011	<0.001	0.0052	0.096	0.12	0.11	**0.14**	**0.25**	**1.7**
CH$_4^{(3)}$ (ppm)	1.90	0.0032 (0.0028)	<0.001	<0.001	0.0051 (0.0055)	0.011	0.0079	**1.90**	**1.91**	**1.0**

*(1) Excluding special events   (2) (X_0 not fixed)   (3) Excluding spike*

1
2   Figure 1: Driving routes in Tartu (top) and Tallinn (bottom). Red line represents: GPS data;

3   Yellow star: stationary measurements location; Blue dots: monitoring stations of the Estonian

4   Environmental Research Institute (EERC).

5

6

7

8

9
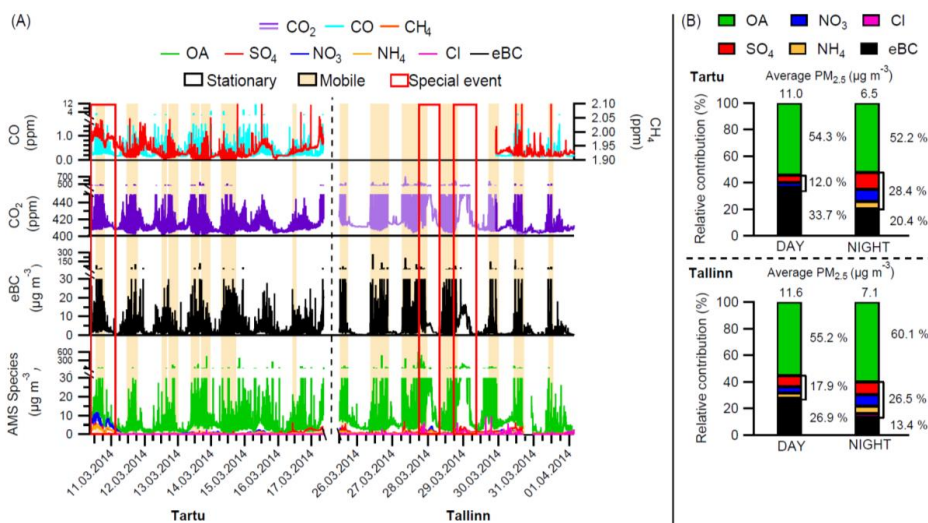
1

2   Figure 2: (a) Temporal evolution of all gas- and particle-phase measured components over

3   the full measurement period; (b) Average $PM_{2.5}$ (NR-$PM_{2.5}$ plus eBC) mass concentration and

4   chemical composition for the measurements in Tartu (top panel) and Tallinn (bottom panel),

5   with day- and night-time distinction.

6

7

8

Atmospheric
Chemistry
and Physics
Discussions
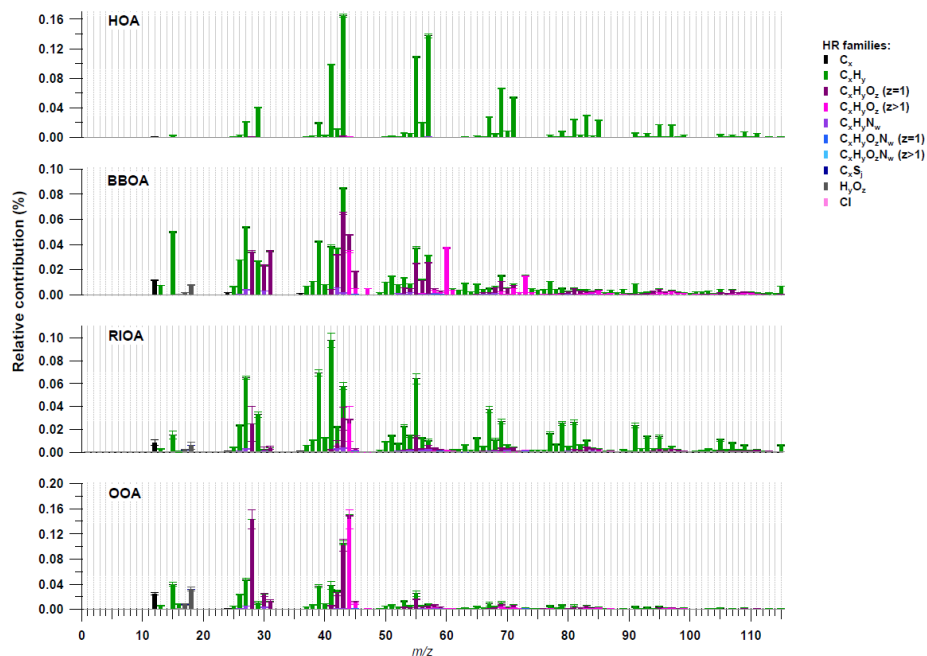
1

2   Figure 3: Mass spectra of the four OA sources identified with PMF. From top to bottom:

3   HOA, BBOA, RIOA and OOA. Error bars indicate the standard deviation among 100

4   bootstrap runs.

5

6

7

8

9

Atmospheric
Chemistry
and Physics

Discussions
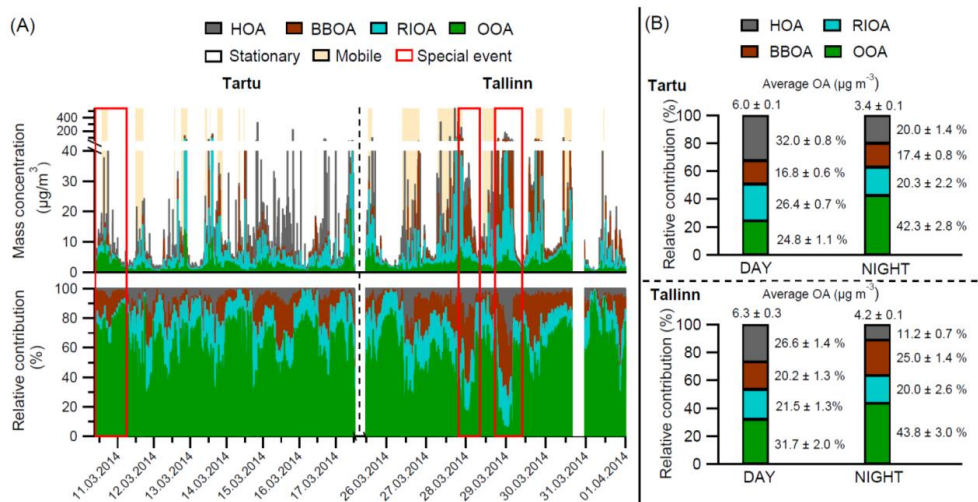
1

2 Figure 4: (a) Temporal evolution of the absolute mass (top panel) and relative contributions

3 (bottom panel) of the four OA sources over the full measurement period; (b) Average OA

4 mass concentrations and relative contributions of the OA sources for the measurements in

5 Tartu (top panel) and Tallinn (bottom panel), with day- and night-time distinction. Errors

6 indicate the standard deviation among 100 bootstrap runs.

7

8

9

Atmospheric
Chemistry
and Physics
Discussions
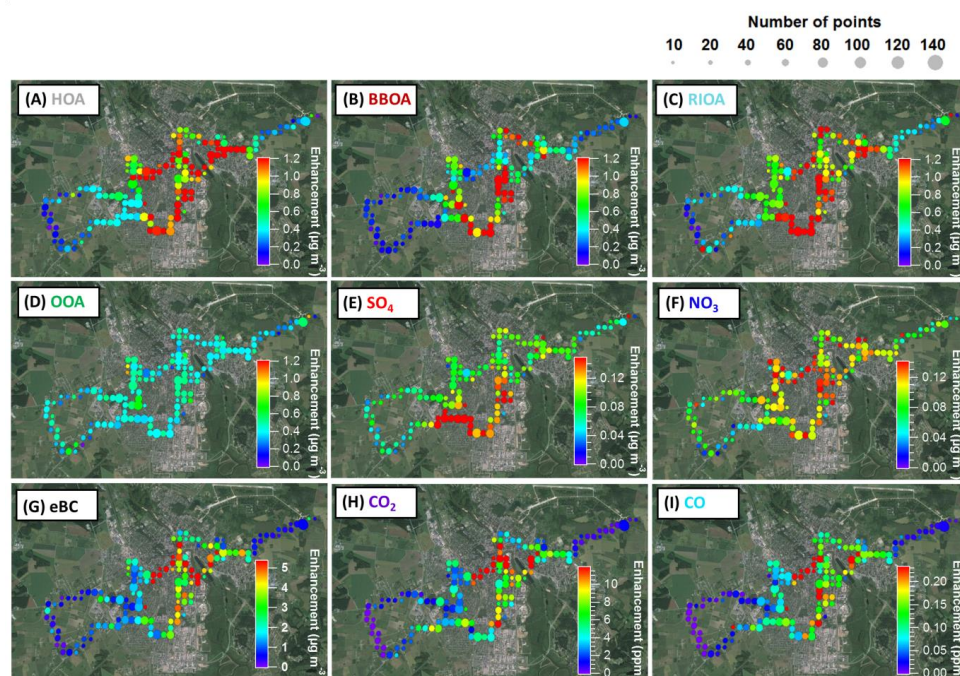
1

2   Figure 5: Average spatial distributions of all identified OA sources (panels a-d) and other

3   measured components (panels e-i) in Tartu. The color scales represent enhancement over the

4   background concentrations; the maximum of the color scales have been fixed to the 75th

5   percentile of the average enhancement of each component in panels e-i and to the highest 75th

6   percentile among all OA sources in panels a-d. The sizes of the points represent the number

7   of points that have been averaged in each case.

8
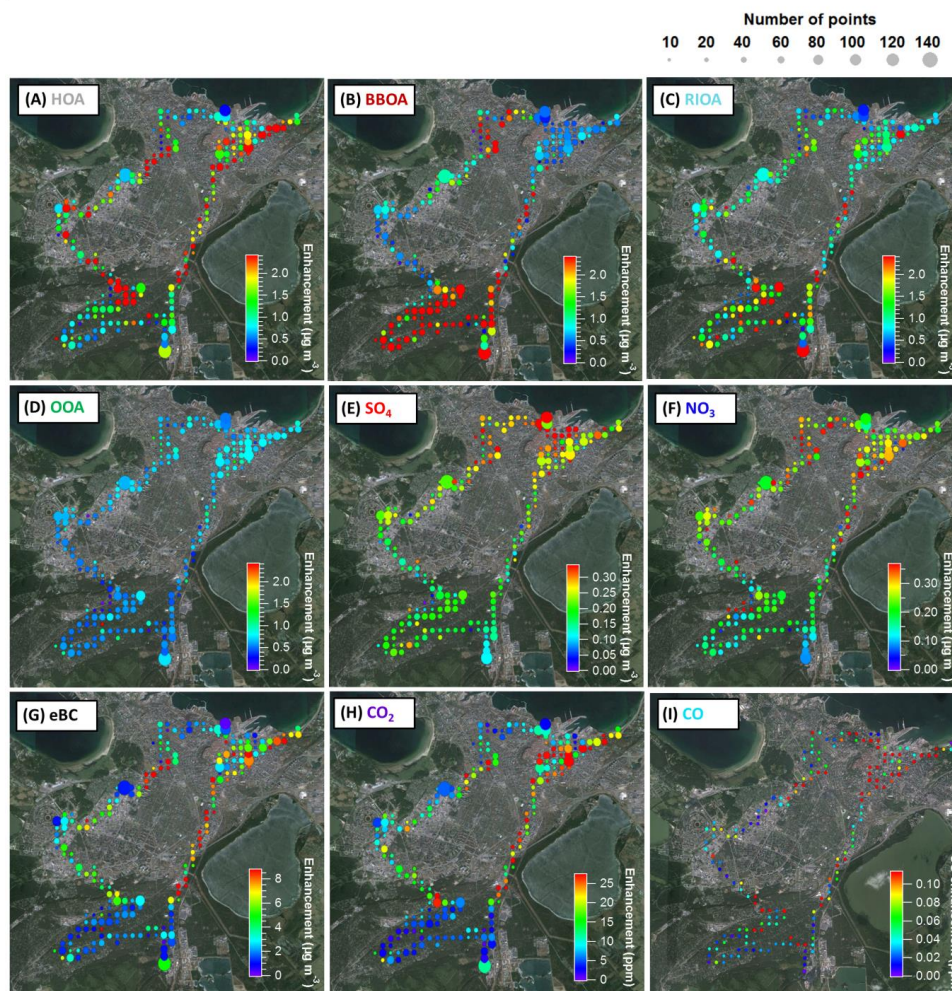
1

2   Figure 6: Average spatial distributions of all identified OA sources (panels a-d) and other

3   measured components (panels e-i) in Tallinn. The color scales represent enhancement over

4   the background concentrations; the maximum of the color scales have been fixed to the 75th

5   percentile of the average enhancement of each component in panels e-i and to the highest 75th

6   percentile among all OA sources in panels a-d. The sizes of the points represent the number

7   of points that have been averaged in each case (Note: less data available for CO).

8

9

10

11

12

Atmospheric
Chemistry
and Physics
Discussions
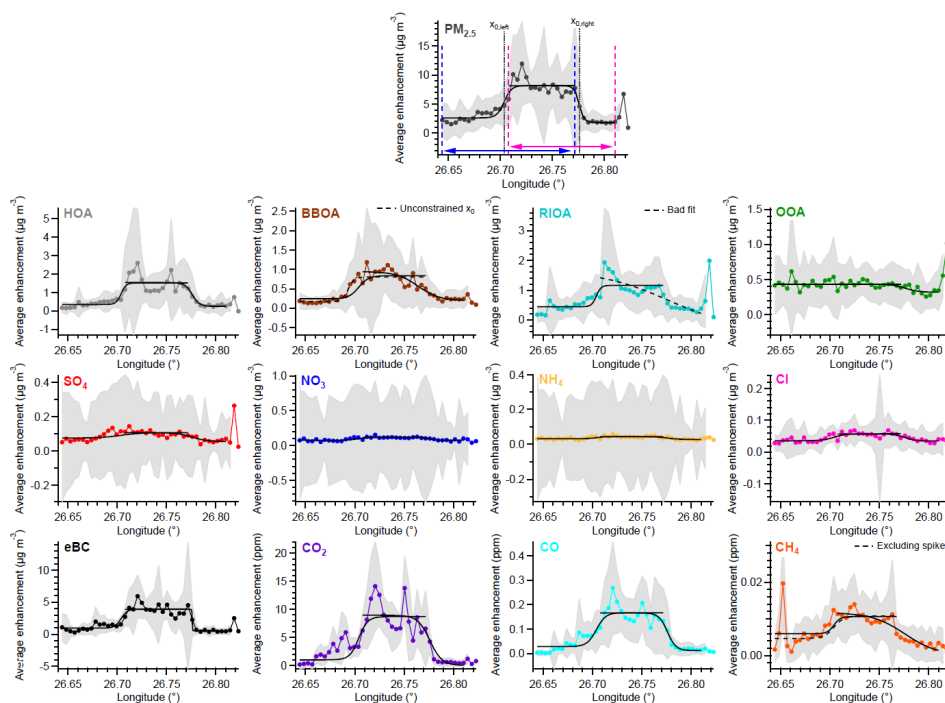
1
2   Figure 7: Average longitude profiles of the enhancements of all measured components and
3   sources in Tartu. Colored curves represent the average enhancement of each
4   source/components over 26 loops and the grey shaded area is the standard deviation among
5   them. The average enhancements were fitted with sigmoid functions (black curves). The
6   fitting limits (pink and blue arrows in top panel) and the sigmoid's midpoint (X_0) were
7   determined from the fit of the total $PM_{2.5}$ mass (NR-$PM_{2.5}$ plus eBC) and then imposed to the
8   other components/sources. Dashed black lines indicate a non-standard fit (described in each
9   case in the plot) and the results of these fits are represented in parenthesis and grey color in
10 Table 2. Notes: The spike found in the east for RIOA, OOA and SO_4 is not representative, as
11 it is related to one single measurement point. The spike in CH_4 in the west side is related to
12 consistent increases of this component nearby a cowshed and will be further investigated in a
13 future publication.
14
15
16
17
18

Atmospheric
Chemistry
and Physics

Discussions
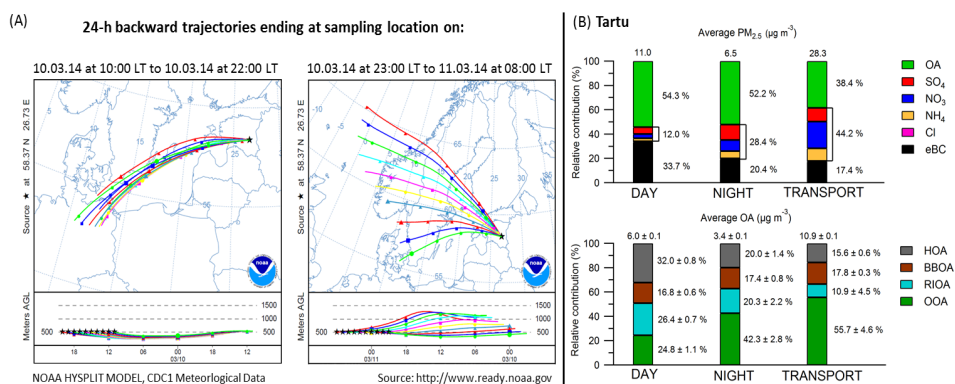
Figure 8: (a) 24-hour back-trajectories (NOAA HYSPLIT MODEL) of the air masses ending at the sampling location (Tartu) during the transport event (left panel) and the successive hours (right panel). (b) PM$_{2.5}$ mass concentration and chemical composition (top panel) and OA mass concentration and relative contributions of the OA sources (bottom panel) during the measurements in Tartu during day-time, night-time and transport event. Errors indicate the standard deviation among 100 bootstrap runs.
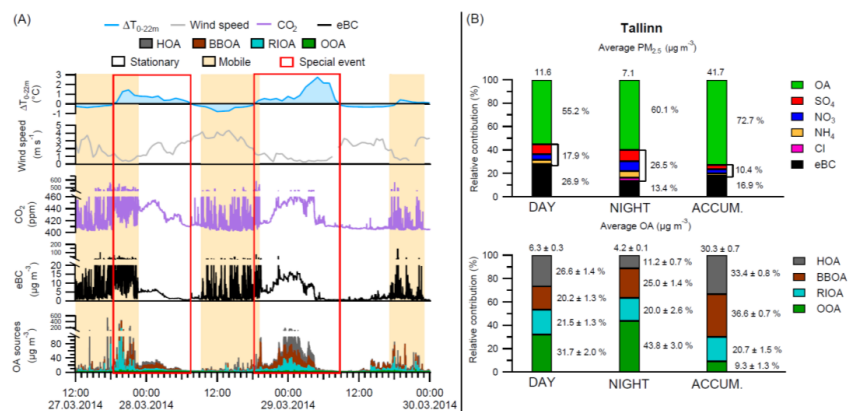
Figure 9: (a) Temporal evolution of the OA sources, eBC and CO_2, wind speed and ΔT_{0-22m} (temperature difference between ground level and at 22 meters above ground level) during the accumulation events in Tallinn. (b) $PM_{2.5}$ mass concentration and chemical composition (top panel) and OA mass concentration and relative contributions of the OA sources (bottom panel) during the measurements in Tallinn during day-time, night-time and accumulation events. Errors indicate the standard deviation among 100 bootstrap runs.